Multi-student Diffusion Distillation for Better One-step Generators

Yanke Song [1] **Jonathan Lorraine** [2 3] **Weili Nie** [2] **Karsten Kreis** [2] **James Lucas** [2]

Abstract

Foundation models that generate photorealistic video with text or image guidance promise compelling augmented-reality (AR) experiences, yet their prohibitive test-time compute prevents true real-time deployment. We focus on the dominant diffusion family and show that Multi-Student Distillation (MSD) increases effective model capacity without increasing — or even reducing — latency, memory footprint, or energy per sample. MSD partitions the conditioning space and trains a lightweight one-step generator per partition, allowing (i) higher sample quality at fixed latency and (ii) smaller per-student backbones for edge/low-latency budgets. MSD advances the agenda of efficient systems for foundation-model training and inference. By attacking the test-time compute bottleneck for diffusion, it is a concrete step toward always-on, on-device AR, which is an emerging and important modality.

1. Introduction

Real-time, high-fidelity video generation is missing for immersive augmented-reality (AR) applications such as live scene re-texturing, telepresence, and interactive storytelling. Diffusion-based foundation models currently set the quality bar for image and video synthesis. Still, they are notoriously slow: hundreds of large network evaluations per clip frame translate into multi-second latencies. This calls for research that reduces large models' compute, time, memory, bandwidth, and energy requirements – especially in new modalities like real-time video.

Knowledge-distillation approaches have made impressive progress, collapsing diffusion sampling to one network evaluation. Unfortunately, performance is tethered to the teacher's heavy backbone: shrinking the student for mobile budgets is impossible or sharply degrades quality, creating a quality–speed dilemma blocking AR deployment.

[1]Department of Statistics, Harvard University, Boston, MA, USA [2]NVIDIA, Santa Clara, CA, USA [3]Vector Institute. Correspondence to: Yanke Song <ysong@g.harvard.edu>, James Lucas <jalucas@nvidia.com>.

We tackle this dilemma with **Multi-Student Distillation (MSD)**. Inspired by mixture-of-experts routing, MSD divides the conditioning space (e.g., class labels or CLIP embeddings) into K semantically coherent shards and trains an independent one-step student on each shard. At inference, a lightweight router selects exactly one student, so total latency equals a single forward pass while aggregate capacity scales with K. Crucially, MSD is orthogonal to recent solver, scheduler, and quantization advances: it can be layered on top of any single-step distillation recipe.

We make three contributions aligning with our interest in test-time compute and emerging real-time modalities:

- **Capacity without latency:** With four same-sized students MSD pushes ImageNet-64 FID to 1.20, surpassing the teacher while preserving latency.
- **Lightweight students:** Adding a lightweight score-matching pre-stage lets MSD distill smaller backbones that cut latency with only minor quality loss—illustrating a compute–quality trade-off tunable to device constraints.
- **Plug-and-play adoption:** MSD is a drop-in wrapper around any conditional single-step distillation pipeline; no architecture changes or extra inference passes required.

Together, these results demonstrate a practical path toward always-on, high-quality AR video—an application that epitomizes our vision of efficient foundation-model systems.

2. Related Work and Background

Due to space constraints, related work on (a) Diffusion sampling acceleration, (b) Mixture of experts training and distillation, and (c) Efficient architectures for diffusion models, are discussed in App. Sec H. Further, background is discussed in App. Sec. I, starting with the background on diffusion models in Sec. I.1 and distribution matching distillation (DMD) in Sec. I.2 followed by how applying adversarial losses to improve distillation in Sec. I.3.

3. Method

In Sec. 3.1, we introduce the general Multi-Student Distillation (MSD) framework that is conceptually applicable to any distillation method. In Sec. 3.2, we show how MSD is applied to distribution matching and adversarial distillation. In Sec. 3.3, we introduce an additional training stage enabling distilling into smaller students.

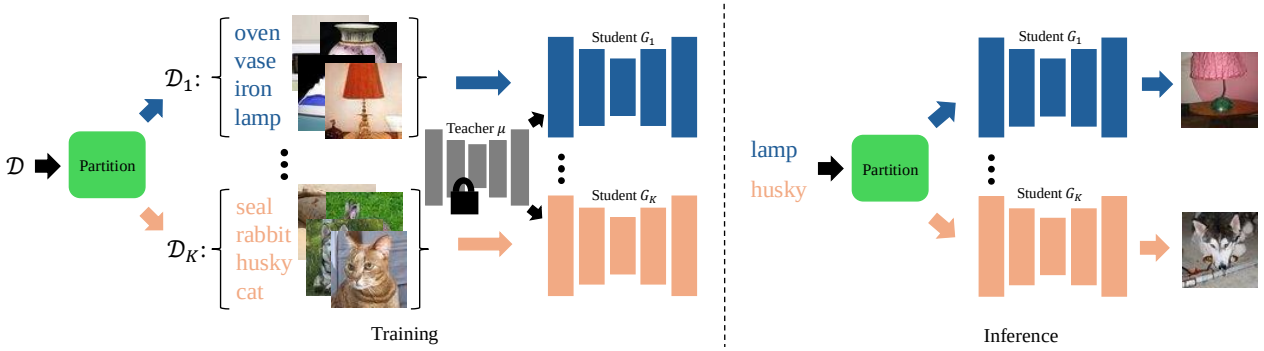

Figure 1: We visualize distilling into multiple students, where each student handles a subset of the input condition. Students are trained separately with filtered data. At inference, 1 student is retrieved for generation given the input condition.

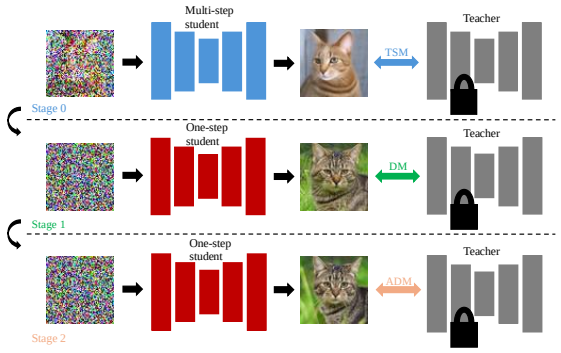

Figure 2: 3-stage training scheme in Eq. 4. Acronym meanings: TSM: teacher score matching (Eq. 3 & Eq. 4); DM: distribution matching (Eq. 4 & Sec. I.2); ADM: adversarial distribution matching (Eq. 4 and Sec. I.3). Stage 1 and Stage 2 are techniques from prior works with same-sized students; Stage 0 is our contribution, which is required for smaller students who cannot initialize with teacher weights.

3.1. Distilling into multiple students

We present Multi-Student Distillation (MSD), a general drop-in framework to with any conditional single-step diffusion distillation method, enabling a cheap upgrade of model capacity without impairing inference speed. We first identify key components of a single-step diffusion distillation framework and then present the modification of MSD. In the vanilla one-student distillation, we have a pretrained teacher denoising diffusion model $\boldsymbol{\mu}_{\text{teacher}}$, a training dataset $\mathcal{D}$, and a distillation method. The distillation yields a single-step generator $G(\boldsymbol{z}; y \in \mathcal{Y})$ via $G = \text{Distill}(\boldsymbol{\mu}_{\text{teacher}}; \mathcal{D})$. The obtained generator G maps a random latent $\boldsymbol{z}$ and an input condition y into an image. In comparison, in an MSD scheme, we instead distill the teacher into K different one-step generators $\{G_k(\boldsymbol{z}; y \in \mathcal{Y}_k)\}_{k=1}^K$ via

$$G_k = \text{Distill}(\mu_{\text{teacher}}, \mathcal{D}_k = F(\mathcal{D}, \mathcal{Y}_k)) \quad (1)$$

with $k = 1, ..., K$. Specifically, each distilled student G_k is specialized in handling a partitioned subset $\mathcal{Y}_k$ of the whole input condition set $\mathcal{Y}$. So, it is trained on a subset of the training data $\mathcal{D}_k \subset \mathcal{D}$, determined by $\mathcal{Y}_k$ via a filtering function F. Fig. 1 illustrates this idea. The partition of $\mathcal{Y}$ into $\{\mathcal{Y}_k\}_{k=1}^K$ determines the input condition groups for which each student is responsible. As a starting point, we make the following three simplifications for choosing a partition: *Disjointness*: This prevents potential redundant training and redundant usage of model capacity. *Equal size*: Since students have the same architecture, the partitions $\{\mathcal{Y}_k\}_{k=1}^K$ should be of equal size that require similar model capacity. *Clustering*: Conditions within each partition should be more similar than those in other partitions, so networks require less capacity to achieve a set quality on their partition.

The first two conditions can be easily satisfied in practice, while the third is not straightforward. For a class-conditional generation, partitioning by semantically similar and equal-sized classes serves a straightforward strategy, though extending it to text-conditional generation is nontrivial. Another promising strategy uses pretrained embedding layers such as the CLIP (Radford et al., 2021) embedding layer or the teacher embedding layer. One could find embeddings of the input conditions and then perform clustering on those embeddings, which are fixed-length numerical vectors containing implicit semantic information. We ablate partition strategies in Sec. B.1. The data filtering function F determines the training subset data $\mathcal{D}_k$ from $\mathcal{Y}_k$. For example, a vanilla filtering strategy could set $F(\mathcal{D}, \mathcal{Y}_k) = \mathcal{D}_k := \mathcal{D}_{\mathcal{Y}_k}$, where $\mathcal{D}_{\mathcal{Y}_k}$ denotes the subset of the training dataset $\mathcal{D}$ that contains the desired condition $\mathcal{Y}_k$. Empirically, we found that this filtering works in most cases, although sometimes a different approach is justified, as demonstrated in Sec. 3.2.

3.2. MSD with distribution matching

As a concrete example, we demonstrate the MSD framework using distribution matching (DM) and adversarial distillation techniques. Inspired by the two-stage framework in (Yin et al., 2024a), each of our students is trained with a distribution matching scheme at the first stage and finetuned with an additional adversarial loss at the second stage (adversarial distribution matching, or ADM):

$$\begin{aligned} G_k^{(1)} &= \text{Distill}_{\text{DM}}\left(\boldsymbol{\mu}_{\text{teacher}}, F_{\text{DM}}(\mathcal{D}_{\text{DM}}, \mathcal{Y}_k)\right), \\ G_k^{(2)} &= \text{Distill}_{\text{ADM}}(\boldsymbol{\mu}_{\text{teacher}}, F_{\text{ADM}}(\mathcal{D}_{\text{ADM}}, \mathcal{Y}_k); G_k^{(1)}), \end{aligned} \quad (2)$$

where we recall that $\boldsymbol{\mu}_{\text{teacher}}$ is the teacher diffusion model, $G_k^{(i)}, k = 1, ..., K$ is the k-th student generator at the i-th stage, F is the data filtering function, $\mathcal{D}$ is the training data, and $\mathcal{Y}_k$ is the set of labels that student k is responsible of.

The first stage $\text{Distill}_{\text{DM}}$ uses distribution matching with a complemented regression loss or the TTUR, with details in Sec. I.2. These methods achieve optimal training efficiency among other best-performing single-step distillation methods (Xie et al., 2024a; Zhou et al., 2024; Kim et al., 2024) without an adversarial loss, with a detailed comparison in App. B.5. The second stage $\text{Distill}_{\text{ADM}}$ adds an adversarial loss (details in Sec. I.3), introducing minimal additional computational overhead and allows resuming from the first stage checkpoint, making it a natural choice.

Designing the training data From Sec. I, the data required for DM and ADM are $\mathcal{D}_{\text{DM}} = (\mathcal{D}_{\text{paired}}, \mathcal{C})$ and $\mathcal{D}_{\text{ADM}} = (\mathcal{D}_{\text{real}}, \mathcal{C})$, where $\mathcal{D}_{\text{paired}}, \mathcal{D}_{\text{real}}, \mathcal{C}$ represents generated paired data, real data and conditional input, respectively. We now discuss choices for the filtering function. For the first stage data filtering F_{DM}, we propose $F_{\text{DM}}(\mathcal{D}_{\text{DM}}, \mathcal{Y}_k) = (\mathcal{D}_{\text{paired}}, \mathcal{C}_{\mathcal{Y}_k})$, where $\mathcal{C}_{\mathcal{Y}_k}$ denotes the subset of condition inputs $\mathcal{C}$ that contains $\mathcal{Y}_k$. That it, we sample all input conditions only on the desired partition for the KL loss but use the whole paired dataset for the regression loss. This special filtering is based on the observation that the size of $\mathcal{D}_{\text{paired}}$ critically affects the terminal performance of DMD distillation: using fewer pairs causes mode collapse, whereas using more pairs challenge the model capacity. Naïvely filtering paired datasets by partition reduces the data size for each student and leads to worse performance, as in our ablation in App. B.4. Instead of generating more paired data to mitigate this imbalance, we simply reuse the original paired dataset for the regression loss. This is remarkably effective, which we hypothesize is because paired data from other input conditions provides effective gradient updates to the shared weights in the network. For the second stage, we stick to the simple data filtering $F_{\text{ADM}}(\mathcal{D}_{\text{ADM}}, \mathcal{Y}_k) = (\mathcal{D}_{\text{real},\mathcal{Y}_k}, \mathcal{C}_{\mathcal{Y}_k})$, so both adversarial and KL losses focus on the specific partition, given each student has enough mode coverage from the first stage.

3.3. Distilling smaller students from scratch

Via the frameworks presented in the last two sections, MSD enables a performance upgrade over alternatives for one student with the same model architecture. In this section, we investigate training multiple students with smaller architectures – and thus faster inference time – without impairing performance much. However, this requires distilling into a student with a different architecture, preventing initialization from pretrained teacher weights. Distilling a single-step student from scratch has been difficult (Xie et al., 2024a), and we could not obtain competitive results with the simple pipeline in Eq. 2. So, we propose an additional pretraining phase $\text{Distill}_{\text{TSM}}$, with TSM denoting Teacher Score Matching, to find a good initialization for single-step distillation. TSM employs the following score-matching loss:

$$\mathcal{L}_{\text{TSM}} = \mathbb{E}_t[\lambda_t \|\boldsymbol{\mu}^{\varphi}_{\text{TSM}}(\boldsymbol{x}_t, t) - \boldsymbol{\mu}_{\text{teacher}}(\boldsymbol{x}_t, t)\|_2^2], \quad (3)$$

where the smaller student with weights φ is trained to match the teacher's score on real images at different noise levels. This step provides useful initialization weights for single-step distillation and is crucial to ensure convergence. With TSM added, the whole pipeline now becomes:

$$\begin{aligned} \boldsymbol{\mu}^{(0)} &= \text{Distill}_{\text{TSM}}\left(\boldsymbol{\mu}_{\text{teacher}}, \mathcal{D}_{\text{real}}\right), \\ G_k^{(1)} &= \text{Distill}_{\text{DM}}(\boldsymbol{\mu}_{\text{teacher}}, F_{\text{DM}}(\mathcal{D}_{\text{DM}}, \mathcal{Y}_k); \boldsymbol{\mu}^{(0)}), \\ G_k^{(2)} &= \text{Distill}_{\text{ADM}}(\boldsymbol{\mu}_{\text{teacher}}, F_{\text{ADM}}(\mathcal{D}_{\text{ADM}}, \mathcal{Y}_k); G_k^{(1)}), \end{aligned} \quad (4)$$

for $k = 1, ..., K$. Although a smaller student may not perfectly match the teacher's score, it still provides a good initialization for stages 1 and 2. The performance gap is remedied in the latter stages by focusing on a smaller partition for each student. This three-stage training scheme is illustrated in Fig. 2.

4. Experiments

To evaluate the effectiveness of our approach, we compared MSD with different design choices against competing methods, including other single-step distillation methods. In Sec. 4.1, we investigate class-conditional image generation on ImageNet-64×64 (Deng et al., 2009) where we have naturally defined classes to partition. Here we explored training with the DM stage only, with both DM and ADM stages, and with all three stages for smaller students. We then evaluate MSD for a larger model in Sec. 4.2. We explored text-to-image generation using MS-COCO2014 (Lin et al., 2014) with varying training stages. We use the standard Fréchet Inception Distance (FID) (Heusel et al., 2017) score and CLIP (Radford et al., 2021) score to measure generation quality. Comprehensive comparisons confirm that MSD outperforms single-student counterparts and sets new records for respective single-step diffusion distillation methods. Finally, in Sec. B.1, we summarize our ablation experiments over design choices. To focus on the performance boost from multi-student distillation, we applied minimal changes to the hyperparameters used by Yin et al. (2024b;a) for their distribution matching distillation implementations. More details on training and evaluation can be found in the App. D and E. In App. A.2, we additionally compare single vs multiple students on a 2D toy problem for direct visual comparison, where we also showcase the applicability of MSD on consistency distillation (Song et al., 2023).

4.1. Class-conditional Image Generation

Student architecture the same as the teacher: We trained $K = 4$ students using the MSD framework and the EDM (Karras et al., 2022) teacher on class-conditional ImageNet-64×64 generation. We applied the simplest strategy for splitting classes among students: Each student is responsible for 250 consecutive classes in numerical order (i.e., $1/K$ of the 1000 classes). We compare the performance with previous methods and display the results in Tab. 1. Our DM

stage, which uses the complementary regression loss, surpasses the one-student counterpart DMD (Yin et al., 2024b), achieving a modest drop of 0.25 in FID score, making it a strong competitor in single-step distillation without an adversarial loss. We then took the best pretrained checkpoints and trained with the ADM stage. The resulting model achieved an FID score of 1.20. It surpasses even the EDM teacher, StyleGAN-XL (Sauer et al., 2022), the multi-step RIN (Jabri et al., 2023) due to the adversarial loss. Fig. 9(b) displays our best student sample generation, with comparable quality as the teacher in Fig. 9(a).

Student architecture smaller than the teacher: Next, we trained 4 smaller student models with the prepended teacher score matching (TSM) stage from Sec. 3.3. This achieved a 42% reduction in model size and a 7% reduction in latency, with a slight degradation in FID score, offering a flexible way to increase generation speed by reducing student size, and increase generation quality by training more students. Fig. 9(c) displays samples from these smaller students, whereas Fig. 9(d) shows samples from an even smaller set of students, with a 71% reduction in model size and a 23% reduction in latency. We observed slightly degraded but still competitive generation qualities. Using more and larger students will further boost performance, as shown by ablations in Sec. B.1 and App. B.6. Smaller students without the TSM stage fail to reach even proper convergence. Instead of the TSM stage, we performed post-output distillation on the best single-step checkpoints and observed a significant performance drop. Hence, the TSM stage is both necessary and efficient.

4.2. Text-to-Image Generation

Student architecture the same as the teacher: We evaluated the performance of text-to-image generation using the MS-COCO2014 (Lin et al., 2014) evaluation dataset. We distilled 4 students from Stable Diffusion (SD) v1.5 (Rombach et al., 2022) on a 5M-image subset of the COYO dataset (Byeon et al., 2022). For splitting prompts among students, we again employed a minimalist design: pass the prompts through the pre-trained SD v1.5 text encoder, pool the embeddings over the temporal dimension, and divide into 4 disjoint subsets along 4 quadrants. We trained with a classifier-free guidance (CFG) scale of 1.75 for best FID performance. Tab. 2 compares the evaluation results with previous methods. Our baseline method with only the DM stage again achieved a performance boost with a 0.48 drop in FID over the single-student counterpart DMD2 without adversarial loss (Yin et al., 2024a). Continuing the ADM stage from the best checkpoint yielded a terminal FID of 8.20, again surpassing the single-student counterpart and setting a new record FID score. In addition, for better visual quality, we also train SD v1.5 and SDXL students with a larger CFG scale of 8, and display corresponding samples in Fig. 3(a), Fig. 14 (SD v1.5) and Fig. 16, Fig. 15, Fig. 11 (SDXL), respectively.

(a) Same-sized student (b) 83% smaller student

Figure 3: Samples on high guidance-scale text-to-image generations from different sized students distilled from the SD v1.5 teacher (full details in App. D). The same-sized student has comparable quality to the teacher (see Fig. 10). The smaller student, trained on a subset of dog-related data, generates faster with decent quality. The same-sized student is trained with DM stage only, while the smaller student is trained with TSM and DM stages (see Fig. 2).

Student architecture smaller than the teacher: To explore the prepended teacher score matching (TSM) stage, we train a 83% smaller and 5% faster student on a dog-related prompt subset of COYO (containing $\sim 1\,210\,000$ prompts). We use a CFG scale of 8 and display the samples in Fig. 3, observing fair generation quality despite a significant drop in model size. Improved training is likely to obtain better sample quality and generalization power. Due to limited computational resources and the complete coverage of the prompt set by the 4-student model, we did not train the full set of students at this size.

Ablation Studies are in App. Sec. B.1 on splitting strategies, number of students, distillation method choice, and more.

5. Discussion

Due to space constraints, limitations are discussed in App. Sec. J.1. This work presented Multi-Student Distillation, a simple yet efficient method to increase the effective model capacity for single-step diffusion distillation. We applied MSD to the distribution matching and adversarial distillation methods. We demonstrated their superior performance over single-student counterparts in both class-conditional generation and text-to-image generation. Particularly, MSD with DMD2's the two-stage training achieves state-of-the-art FID scores. Moreover, we successfully distilled smaller students from scratch, demonstrating MSD's potential in further reducing the generation latency with multiple smaller student distillations. We envision building on MSD to enable generation in real-time, enabling many new use cases.

Table 1: Comparing class-conditional generators on ImageNet-64×64. The number of function evaluations (NFE) for MSD is 1 as a single student is used at inference for the given input.

Method	NFE (↓)	FID (↓)
Multiple Steps		
RIN (Jabri et al., 2023)	1000	1.23
ADM (Dhariwal and Nichol, 2021)	250	2.07
DPM Solver (Lu et al., 2022a)	10	7.93
Multistep CD (Heek et al., 2024)	2	2.0
Single Step, w/o GAN		
PD (Salimans and Ho, 2022)	1	15.39
DSNO (Zheng et al., 2023)	1	7.83
Diff-Instruct (Luo et al., 2024)	1	5.57
iCT-deep (Song and Dhariwal, 2024)	1	3.25
Moment Matching (Salimans et al., 2024)	1	3.0
DMD (Yin et al., 2024b)	1	2.62
MSD (ours): 4 students, DM only	1	2.37
EMD (Xie et al., 2024a)	1	2.20
SiD (Zhou et al., 2024)	1	1.52
Single Step, w/ GAN		
Post-distillation, 4, 42% smaller students	1	11.67
MSD (ours): 4, 42% smaller students, ADM	1	2.88
StyleGAN-XL (Sauer et al., 2022)	1	1.52
CTM (Kim et al., 2024)	1	1.92
DMD2 (Yin et al., 2024a)	1	1.28
MSD (ours): 4 students, ADM	1	1.20
teacher		
EDM (teacher, ODE) (Karras et al., 2022)	511	2.32
EDM (teacher, SDE) (Karras et al., 2022)	511	1.36

Table 2: Comparing MSD on zero-shot text-to-image generation on MS-COCO2014. We measure speed with sampling time per prompt (latency) and quality with FID.

Method	Latency (↓)	FID (↓)
Unaccelerated		
DALL·E 2 (Ramesh et al., 2022)	-	10.39
LDM (Rombach et al., 2022)	3.7s	12.63
eDiff-I (Balaji et al., 2022)	32.0s	6.95
GANs		
StyleGAN-T (Sauer et al., 2023a)	0.10s	12.90
GigaGAN (Yu et al., 2022)	0.13s	9.09
Accelerated		
DPM++ (4 step) (Lu et al., 2022b)	0.26s	22.36
InstaFlow-0.9B (Liu et al., 2023a)	0.09s	12.10
UFOGen (Xu et al., 2024)	0.09s	12.78
DMD (Yin et al., 2024b)	0.09s	11.49
EMD (Xie et al., 2024a)	0.09s	9.66
DMD2 (w/o GAN)	0.09s	9.28
MSD (ours): 4 students, DM only	0.09s	8.80
DMD2 (Yin et al., 2024a)	0.09s	8.35
MSD (ours): 4 students, ADM	0.09s	8.20
teacher		
SDv1.5 (50 step, CFG=3, ODE)	2.59s	8.59
SDv1.5 (200 step, CFG=2, SDE)	10.25s	7.21

References

Alec Radford, Jong Wook Kim, Chris Hallacy, Aditya Ramesh, Gabriel Goh, Sandhini Agarwal, Girish Sastry, Amanda Askell, Pamela Mishkin, Jack Clark, et al. Learning transferable visual models from natural language supervision. In *International conference on machine learning*, pages 8748–8763. PMLR, 2021. 2, 3

Tianwei Yin, Michaël Gharbi, Taesung Park, Richard Zhang, Eli Shechtman, Fredo Durand, and William T Freeman. Improved distribution matching distillation for fast image synthesis. *arXiv preprint arXiv:2405.14867*, 2024a. 2, 3, 4, 5, 11, 12, 13, 14, 15, 18, 19

Sirui Xie, Zhisheng Xiao, Diederik P Kingma, Tingbo Hou, Ying Nian Wu, Kevin Patrick Murphy, Tim Salimans, Ben Poole, and Ruiqi Gao. Em distillation for one-step diffusion models. *arXiv preprint arXiv:2405.16852*, 2024a. 3, 5, 13, 18

Mingyuan Zhou, Huangjie Zheng, Zhendong Wang, Mingzhang Yin, and Hai Huang. Score identity distillation: Exponentially fast distillation of pretrained diffusion models for one-step generation. In *Forty-first International Conference on Machine Learning*, 2024. 3, 5, 13, 18

Dongjun Kim, Chieh-Hsin Lai, Wei-Hsiang Liao, Naoki Murata, Yuhta Takida, Toshimitsu Uesaka, Yutong He, Yuki Mitsufuji, and Stefano Ermon. Consistency trajectory models: Learning probability flow ode trajectory of diffusion. *International Conference on Learning Representations*, 2024. 3, 5, 13, 18

Jia Deng, Wei Dong, Richard Socher, Li-Jia Li, Kai Li, and Li Fei-Fei. Imagenet: A large-scale hierarchical image database. In *2009 IEEE conference on computer vision and pattern recognition*, pages 248–255. Ieee, 2009. 3

Tsung-Yi Lin, Michael Maire, Serge Belongie, James Hays, Pietro Perona, Deva Ramanan, Piotr Dollár, and C Lawrence Zitnick. Microsoft coco: Common objects in context. In *Computer Vision–ECCV 2014: 13th European Conference, Zurich, Switzerland, September 6-12, 2014, Proceedings, Part V 13*, pages 740–755. Springer, 2014. 3, 4

Martin Heusel, Hubert Ramsauer, Thomas Unterthiner, Bernhard Nessler, and Sepp Hochreiter. Gans trained by a two time-scale update rule converge to a local nash equilibrium. *Advances in neural information processing systems*, 30, 2017. 3

Tianwei Yin, Michaël Gharbi, Richard Zhang, Eli Shechtman, Fredo Durand, William T Freeman, and Taesung Park. One-step diffusion with distribution matching distillation. In *Proceedings of the IEEE/CVF Conference on Computer Vision and Pattern Recognition*, pages 6613–6623, 2024b. 3, 4, 5, 11, 12, 13, 14, 15, 18

Yang Song, Prafulla Dhariwal, Mark Chen, and Ilya Sutskever. Consistency models. In *International Conference on Machine Learning*, pages 32211–32252. PMLR, 2023. 3, 10, 18

Tero Karras, Miika Aittala, Timo Aila, and Samuli Laine. Elucidating the design space of diffusion-based generative models. *Advances in neural information processing systems*, 35:26565–26577, 2022. 3, 5, 14, 15, 18

Axel Sauer, Katja Schwarz, and Andreas Geiger. Stylegan-xl: Scaling stylegan to large diverse datasets. In *ACM SIGGRAPH 2022 conference proceedings*, pages 1–10, 2022. 4, 5

Allan Jabri, David J Fleet, and Ting Chen. Scalable adaptive computation for iterative generation. In *Proceedings of the 40th International Conference on Machine Learning*, pages 14569–14589, 2023. 4, 5

Prafulla Dhariwal and Alexander Nichol. Diffusion models beat gans on image synthesis. *Advances in neural information processing systems*, 34:8780–8794, 2021. 5

Cheng Lu, Yuhao Zhou, Fan Bao, Jianfei Chen, Chongxuan Li, and Jun Zhu. Dpm-solver: A fast ode solver for diffusion probabilistic model sampling in around 10 steps. *Advances in Neural Information Processing Systems*, 35: 5775–5787, 2022a. 5, 18

Jonathan Heek, Emiel Hoogeboom, and Tim Salimans. Multistep consistency models. *arXiv preprint arXiv:2403.06807*, 2024. 5

Tim Salimans and Jonathan Ho. Progressive distillation for fast sampling of diffusion models. *International Conference on Learning Representations*, 2022. 5, 18

Hongkai Zheng, Weili Nie, Arash Vahdat, Kamyar Azizzadenesheli, and Anima Anandkumar. Fast sampling of diffusion models via operator learning. In *International conference on machine learning*, pages 42390–42402. PMLR, 2023. 5, 18

Weijian Luo, Tianyang Hu, Shifeng Zhang, Jiacheng Sun, Zhenguo Li, and Zhihua Zhang. Diff-instruct: A universal approach for transferring knowledge from pre-trained diffusion models. *Advances in Neural Information Processing Systems*, 36, 2024. 5, 18

Yang Song and Prafulla Dhariwal. Improved techniques for training consistency models. *International Conference on Learning Representations*, 2024. 5

Tim Salimans, Thomas Mensink, Jonathan Heek, and Emiel Hoogeboom. Multistep distillation of diffusion models via moment matching. *arXiv preprint arXiv:2406.04103*, 2024. 5, 18

Aditya Ramesh, Prafulla Dhariwal, Alex Nichol, Casey Chu, and Mark Chen. Hierarchical text-conditional image generation with clip latents. *arXiv preprint arXiv:2204.06125*, 1(2):3, 2022. 5

Robin Rombach, Andreas Blattmann, Dominik Lorenz, Patrick Esser, and Björn Ommer. High-resolution image synthesis with latent diffusion models. In *Proceedings of the IEEE/CVF conference on computer vision and pattern recognition*, pages 10684–10695, 2022. 4, 5, 12, 14, 15

Yogesh Balaji, Seungjun Nah, Xun Huang, Arash Vahdat, Jiaming Song, Qinsheng Zhang, Karsten Kreis, Miika Aittala, Timo Aila, Samuli Laine, et al. ediff-i: Text-to-image diffusion models with an ensemble of expert denoisers. *arXiv preprint arXiv:2211.01324*, 2022. 5, 18

Axel Sauer, Tero Karras, Samuli Laine, Andreas Geiger, and Timo Aila. Stylegan-t: Unlocking the power of gans for fast large-scale text-to-image synthesis. In *International conference on machine learning*, pages 30105–30118. PMLR, 2023a. 5

Jiahui Yu, Yuanzhong Xu, Jing Yu Koh, Thang Luong, Gunjan Baid, Zirui Wang, Vijay Vasudevan, Alexander Ku, Yinfei Yang, Burcu Karagol Ayan, et al. Scaling autoregressive models for content-rich text-to-image generation. *arXiv preprint arXiv:2206.10789*, 2(3):5, 2022. 5, 15

Cheng Lu, Yuhao Zhou, Fan Bao, Jianfei Chen, Chongxuan Li, and Jun Zhu. Dpm-solver++: Fast solver for guided sampling of diffusion probabilistic models. *arXiv preprint arXiv:2211.01095*, 2022b. 5, 12, 18

Xingchao Liu, Xiwen Zhang, Jianzhu Ma, Jian Peng, et al. Instaflow: One step is enough for high-quality diffusion-based text-to-image generation. In *The Twelfth International Conference on Learning Representations*, 2023a. 5, 18

Yanwu Xu, Yang Zhao, Zhisheng Xiao, and Tingbo Hou. Ufogen: You forward once large scale text-to-image generation via diffusion gans. In *Proceedings of the IEEE/CVF Conference on Computer Vision and Pattern Recognition*, pages 8196–8206, 2024. 5, 18

Minwoo Byeon, Beomhee Park, Haecheon Kim, Sungjun Lee, Woonhyuk Baek, and Saehoon Kim. Coyo-700m: Image-text pair dataset. https://github.com/kakaobrain/coyo-dataset, 2022. 4, 10, 14, 15

Wenliang Zhao, Lujia Bai, Yongming Rao, Jie Zhou, and Jiwen Lu. Unipc: A unified predictor-corrector framework for fast sampling of diffusion models. *Advances in Neural Information Processing Systems*, 36, 2024. 12

Simian Luo, Yiqin Tan, Suraj Patil, Daniel Gu, Patrick von Platen, Apolinário Passos, Longbo Huang, Jian Li, and Hang Zhao. Lcm-lora: A universal stable-diffusion acceleration module. *arXiv preprint arXiv:2311.05556*, 2023. 12, 18

Christoph Schuhmann, Romain Beaumont, Richard Vencu, Cade Gordon, Ross Wightman, Mehdi Cherti, Theo Coombes, Aarush Katta, Clayton Mullis, Mitchell Wortsman, et al. Laion-5b: An open large-scale dataset for training next generation image-text models. *Advances in Neural Information Processing Systems*, 35:25278–25294, 2022. 10

I Loshchilov. Decoupled weight decay regularization. *arXiv preprint arXiv:1711.05101*, 2017. 13, 14

Richard Zhang, Phillip Isola, Alexei A Efros, Eli Shechtman, and Oliver Wang. The unreasonable effectiveness of deep features as a perceptual metric. In *Proceedings of the IEEE conference on computer vision and pattern recognition*, pages 586–595, 2018. 14, 19

Shanchuan Lin, Anran Wang, and Xiao Yang. Sdxl-lightning: Progressive adversarial diffusion distillation. *arXiv preprint arXiv:2402.13929*, 2024. 15, 18

Gaurav Parmar, Richard Zhang, and Jun-Yan Zhu. On aliased resizing and surprising subtleties in gan evaluation. In *Proceedings of the IEEE/CVF Conference on Computer Vision and Pattern Recognition*, pages 11410–11420, 2022. 15

Kaiwen Zheng, Cheng Lu, Jianfei Chen, and Jun Zhu. Dpm-solver-v3: Improved diffusion ode solver with empirical model statistics. *Advances in Neural Information Processing Systems*, 36, 2024. 18

Luping Liu, Yi Ren, Zhijie Lin, and Zhou Zhao. Pseudo numerical methods for diffusion models on manifolds. *International Conference on Learning Representations*, 2022. 18

Eric Luhman and Troy Luhman. Knowledge distillation in iterative generative models for improved sampling speed. *arXiv preprint arXiv:2101.02388*, 2021. 18

Chenlin Meng, Robin Rombach, Ruiqi Gao, Diederik Kingma, Stefano Ermon, Jonathan Ho, and Tim Salimans. On distillation of guided diffusion models. In *Proceedings of the IEEE/CVF Conference on Computer Vision and Pattern Recognition*, pages 14297–14306, 2023. 18

Xingchao Liu, Chengyue Gong, and Qiang Liu. Flow straight and fast: Learning to generate and transfer data with rectified flow. *International Conference on Learning Representations*, 2023b. 18

Hanshu Yan, Xingchao Liu, Jiachun Pan, Jun Hao Liew, Qiang Liu, and Jiashi Feng. Perflow: Piecewise rectified flow as universal plug-and-play accelerator. *arXiv preprint arXiv:2405.07510*, 2024. 18

Yuxi Ren, Xin Xia, Yanzuo Lu, Jiacheng Zhang, Jie Wu, Pan Xie, Xing Wang, and Xuefeng Xiao. Hyper-sd: Trajectory segmented consistency model for efficient image synthesis. *arXiv preprint arXiv:2404.13686*, 2024. 18

Thuan Hoang Nguyen and Anh Tran. Swiftbrush: One-step text-to-image diffusion model with variational score distillation. In *Proceedings of the IEEE/CVF Conference on Computer Vision and Pattern Recognition*, pages 7807–7816, 2024. 18

Ian Goodfellow, Jean Pouget-Abadie, Mehdi Mirza, Bing Xu, David Warde-Farley, Sherjil Ozair, Aaron Courville, and Yoshua Bengio. Generative adversarial nets. *Advances in neural information processing systems*, 27, 2014. 18, 19

Zhisheng Xiao, Karsten Kreis, and Arash Vahdat. Tackling the generative learning trilemma with denoising diffusion gans. *International Conference on Learning Representations*, 2022. 18

Bowen Zheng and Tianming Yang. Diffusion models are innate one-step generators. *arXiv preprint arXiv:2405.20750*, 2024. 18

Axel Sauer, Dominik Lorenz, Andreas Blattmann, and Robin Rombach. Adversarial diffusion distillation. *arXiv preprint arXiv:2311.17042*, 2023b. 18

Axel Sauer, Frederic Boesel, Tim Dockhorn, Andreas Blattmann, Patrick Esser, and Robin Rombach. Fast high-resolution image synthesis with latent adversarial diffusion distillation. *arXiv preprint arXiv:2403.12015*, 2024. 18

Zhendong Wang, Huangjie Zheng, Pengcheng He, Weizhu Chen, and Mingyuan Zhou. Diffusion-gan: Training gans with diffusion. *International Conference on Learning Representations*, 2023. 18

Michael I Jordan and Robert A Jacobs. Hierarchical mixtures of experts and the em algorithm. *Neural computation*, 6(2):181–214, 1994. 18

Noam Shazeer, Azalia Mirhoseini, Krzysztof Maziarz, Andy Davis, Quoc Le, Geoffrey Hinton, and Jeff Dean. Outrageously large neural networks: The sparsely-gated mixture-of-experts layer. *International Conference on Learning Representations*, 2017. 18

Dmitry Lepikhin, HyoukJoong Lee, Yuanzhong Xu, Dehao Chen, Orhan Firat, Yanping Huang, Maxim Krikun, Noam Shazeer, and Zhifeng Chen. Gshard: Scaling giant models with conditional computation and automatic sharding. *International Conference on Learning Representations*, 2021. 18

William Fedus, Barret Zoph, and Noam Shazeer. Switch transformers: Scaling to trillion parameter models with simple and efficient sparsity. *Journal of Machine Learning Research*, 23(120):1–39, 2022. 18

Mike Lewis, Shruti Bhosale, Tim Dettmers, Naman Goyal, and Luke Zettlemoyer. Base layers: Simplifying training of large, sparse models. In *International Conference on Machine Learning*, pages 6265–6274. PMLR, 2021. 18

Haitz Sáez de Ocáriz Borde, Takashi Furuya, Anastasis Kratsios, and Marc T Law. Breaking the curse of dimensionality with distributed neural computation. *arXiv preprint arXiv:2402.03460*, 2024. 18

Geoffrey Hinton, Oriol Vinyals, and Jeff Dean. Distilling the knowledge in a neural network. *arXiv preprint arXiv:1503.02531*, 2015. 18

Defang Chen, Jian-Ping Mei, Can Wang, Yan Feng, and Chun Chen. Online knowledge distillation with diverse peers. In *Proceedings of the AAAI conference on artificial intelligence*, volume 34, pages 3430–3437, 2020. 18

Tian Ni and Haoji Hu. Knowledge distillation by multiple student instance interaction. In *2023 International Conference on Pattern Recognition, Machine Vision and Intelligent Algorithms (PRMVIA)*, pages 193–200. IEEE, 2023. 18

Xiaoqin Chang, Sophia Yat Mei Lee, Suyang Zhu, Shoushan Li, and Guodong Zhou. One-teacher and multiple-student knowledge distillation on sentiment classification. In *Proceedings of the 29th International Conference on Computational Linguistics*, pages 7042–7052, 2022. 18

Zhitian Xie, Yinger Zhang, Chenyi Zhuang, Qitao Shi, Zhining Liu, Jinjie Gu, and Guannan Zhang. Mode: A mixture-of-experts model with mutual distillation among the experts. In *Proceedings of the AAAI Conference on Artificial Intelligence*, volume 38, pages 16067–16075, 2024b. 18

Sneha Kudugunta, Yanping Huang, Ankur Bapna, Maxim Krikun, Dmitry Lepikhin, Minh-Thang Luong, and Orhan Firat. Beyond distillation: Task-level mixture-of-experts for efficient inference. In *Findings of the Association for Computational Linguistics: EMNLP 2021*, pages 3577–3599, 2021. 18

Simiao Zuo, Qingru Zhang, Chen Liang, Pengcheng He, Tuo Zhao, and Weizhu Chen. Moebert: from bert to mixture-of-experts via importance-guided adaptation. In *Proceedings of the 2022 Conference of the North American Chapter of the Association for Computational Linguistics: Human Language Technologies*, 2022. 18

Quan Hoang, Tu Dinh Nguyen, Trung Le, and Dinh Phung. Mgan: Training generative adversarial nets with multiple generators. In *International conference on learning representations*, 2018. 18

David Keetae Park, Seungjoo Yoo, Hyojin Bahng, Jaegul Choo, and Noseong Park. Megan: Mixture of experts of generative adversarial networks for multimodal image generation. In *27th International Joint Conference on Artificial Intelligence, IJCAI 2018*, pages 878–884. International Joint Conferences on Artificial Intelligence, 2018. 18

Alper Ahmetoğlu and Ethem Alpaydın. Hierarchical mixtures of generators for adversarial learning. In *2020 25th International Conference on Pattern Recognition (ICPR)*, pages 316–323. IEEE, 2021. 18

Fan Bao, Chongxuan Li, Yue Cao, and Jun Zhu. All are worth words: a vit backbone for score-based diffusion models. In *NeurIPS 2022 Workshop on Score-Based Methods*, 2022. 18

William Peebles and Saining Xie. Scalable diffusion models with transformers. In *Proceedings of the IEEE/CVF International Conference on Computer Vision*, pages 4195–4205, 2023. 18

Emiel Hoogeboom, Jonathan Heek, and Tim Salimans. simple diffusion: End-to-end diffusion for high resolution images. In *International Conference on Machine Learning*, pages 13213–13232. PMLR, 2023. 18

Bo-Kyeong Kim, Hyoung-Kyu Song, Thibault Castells, and Shinkook Choi. On architectural compression of text-to-image diffusion models. 2023. 18

Yanyu Li, Huan Wang, Qing Jin, Ju Hu, Pavlo Chemerys, Yun Fu, Yanzhi Wang, Sergey Tulyakov, and Jian Ren. Snapfusion: Text-to-image diffusion model on mobile devices within two seconds. *Advances in Neural Information Processing Systems*, 36, 2024. 18

Dingkun Zhang, Sijia Li, Chen Chen, Qingsong Xie, and Haonan Lu. Laptop-diff: Layer pruning and normalized distillation for compressing diffusion models. *arXiv preprint arXiv:2404.11098*, 2024. 18

Yang Zhao, Yanwu Xu, Zhisheng Xiao, and Tingbo Hou. Mobilediffusion: Subsecond text-to-image generation on mobile devices. *arXiv preprint arXiv:2311.16567*, 2023. 18

Yang Song, Jascha Sohl-Dickstein, Diederik P Kingma, Abhishek Kumar, Stefano Ermon, and Ben Poole. Score-based generative modeling through stochastic differential equations. *International Conference on Learning Representations*, 2021. 18

Jonathan Ho, Ajay Jain, and Pieter Abbeel. Denoising diffusion probabilistic models. *Advances in neural information processing systems*, 33:6840–6851, 2020. 18

Zhengyi Wang, Cheng Lu, Yikai Wang, Fan Bao, Chongxuan Li, Hang Su, and Jun Zhu. Prolificdreamer: High-fidelity and diverse text-to-3d generation with variational score distillation. *Advances in Neural Information Processing Systems*, 36, 2024. 18

Senmao Ye and Fei Liu. Score mismatching for generative modeling. *Neural Networks*, 175:106311, 2024. 18

Impact Statement

Our work aims to improve the quality and speed of diffusion models, thus we may inherit concerns from diffusion models and generative models in general. Potential risks include fabricating facts that could mislead public opinion, displaying biased information that may amplify social biases, and displacing creative jobs from artists and designers.

A. Additional experimental results

A.1. CLIP score for high guidance scale

Tab. 4 shows the CLIP score of MSD and single-student methods. MSD4-ADM achieves a competitive CLIP score and beats the single student counterpart, DMD2. We believe the CLIP score can increase further if one trains on the LAION dataset (Schuhmann et al., 2022) instead of the COYO dataset (Byeon et al., 2022).

A.2. Toy Experiments

We showcase the advantage of MSD in a 2D toy model, where the performance difference is visually apparent. The real data distribution has 8 classes, and each class is a mixture of 8 Gaussians. We used a simple MLP with EDM schedules to train the teacher and then distill into 1, 2, 4, and 8 students. We applied our DM stage, as well as another distillation method, Consistency Distillation (Song et al., 2023), and display the results in Fig. 4 and Fig. 5, respectively. From the displayed samples and the ℓ_1 distance from teacher generation, we observe that the collective generation quality increases as the number of students increases. This trend is common in both distillation methods, indicating the generality of MSD.

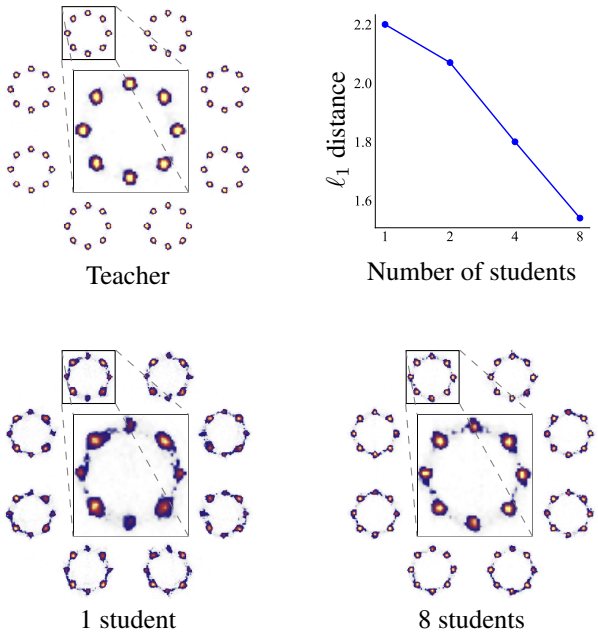

Figure 4: A 2D toy model. From left to right: teacher (multi-step) generation and student, one-step generation with 1 and 8 distilled students, the ℓ_1 distance of generated samples between teacher and students. **Takeaway:** More students improve distillation quality on this easy-to-visualize setup.

B. Extended Ablation studies

B.1. Ablation Studies

Here, we ablate the effect of different components in MSD and offer insight into scaling. Unless otherwise mentioned, all experiments are conducted for class-conditional generation ImageNet-64×64, using only the DM stage for computational efficiency. See additional ablation studies in App. B.

Simple splitting works surprisingly well. We used consecutive splitting of classes in Sec. 4.1. Although it shows obvious advantage over random splitting, as shown in Tab. 5, it does not use the embedding information from the pre-trained EDM model. Therefore, we investigated another strategy where we performed a K-means clustering ($K = 4$) on the label embeddings, resulting in 4 clusters of similar sizes: $(230, 283, 280, 207)$. However, MSD trained with these clustered partitions performs similarly to sequential partition, as shown in Tab. 5. For text-to-image generation, we performed K-means clustering on the pooled embeddings of prompts in the training data, resulting in clusters of vastly uneven sizes. Due to computational limitations, we opted for the simpler partition strategies outlined in Sec. 4.

Effect of scaling the number of students. In Tab. 5, we study the effect of increasing K, the number of students. We kept the per-student batch size fixed so more students induce a larger effective batch size. We observe better FID scores for more students. We hypothesize that better training strategies, such as per-student tuning, will further improve the quality. Optimal strategies for scaling to ultra-large numbers of students is an interesting area for future work.

B.2. MSD is Still Better with the Same Effective Batch Size

To investigate if the performance boost from MSD comes from only a batch size increase over single student distillation, we make a comparison with the same effective batch size. As showcased in Tab. 5, MSD with 4 students and a batch size of 32 per student performs slightly better than the single-student counterpart with a batch size of 128, indicating that MSD likely benefits from a capacity increase than a batch size increase. As a takeaway, with a fixed training resource measured in processed data points, users are better off distilling into multiple students with partitioned resources each than using all resources to distill into a single student. This is also reflected in our previous experiments, where we used significantly less resources per student than

Table 3: Glossary and notation

MSD	Multi-student distillation
DM	Distribution Matching
ADM	Distribution Matching with Adversarial loss
TSM	Teacher Score Matching
MoE	Mixture of experts
DMD	Distribution Matching Distillation (Yin et al., 2024b)
DMD2	Improved Distribution Matching Distillation (Yin et al., 2024a)
SOTA	State-of-the-art
FID	Fréchet Inception Distance
LPIPS	Learned Perceptual Image Patch Similarity
NFE	Number of Function Evaluations
SD	Stable Diffusion
TTUR	Two-Timescale Update Rule
CFG	Classifier-free guidance
MLP	Multi-layer Perceptron
GAN	Generative Adversarial Network
SDE/ODE	Stochastic/Ordinary Differential Equation
$i, j, k, n \in \mathbb{N}$	Indices
$I, J, K, N \in \mathbb{N}$	Sizes
$x, y, z \in \mathbb{R}$	Scalars
$\boldsymbol{x}, \boldsymbol{y}, \boldsymbol{z} \in \mathbb{R}^N$	Vectors
$\boldsymbol{X}, \boldsymbol{Y}, \boldsymbol{Z} \in \mathbb{R}^{N \times N}$	Matrices
$\mathcal{X}, \mathcal{Y}, \mathcal{Z}$	Sets / domains
$\boldsymbol{I}$	The identity matrix
G	Single-step generator
φ	Student network weights
ϕ	"fake" score network weights
ℓ_1	Manhattan distance
Distill	Distillation method
μ	Denoising network
K	Number of students
k	Student index
(i)	Distillation stage
$\mathcal{D}$	Dataset
$\mathcal{C}$	Condition dataset (without images)
$\mathcal{Y}$	The abstract condition set
F	Filtering function on input conditions

the single-student counterparts (see details in App. D). Although multiple students means multiple model weights to save, storage is often cheap, so in many applications, this cost is outweighed by our improved quality or latency.

B.3. Training curves for Sec. B.1

Fig. 6 displays the training curves for the ablation studies shown in Tab. 5. The relative terminal performances are also reflected in the training process.

B.4. The effect of paired dataset size on DMD

In Sec. 3.2, we mentioned the special filtering strategy for MSD at DM stage: instead of partitioning the paired dataset for corresponding classes, we choose to keep the same complete dataset for each student. Fig. 7 demonstrates that the alternative strategy discourages mode coverage and leads to a worse terminal performance.

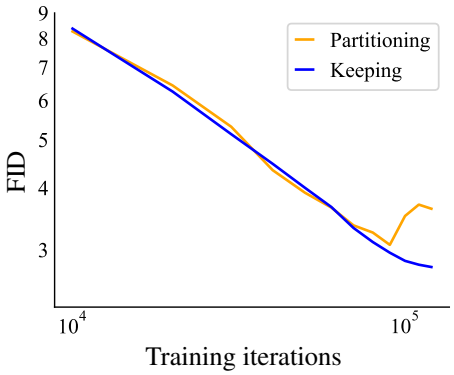

Figure 7: Comparison of paired dataset filtering strategies for MSD4-DM. Partitioning the paired dataset for each student discourages mode coverage, which results in worse terminal performance. In comparison, keeping the same paired dataset for each student achieves better performance without impairing the convergence speed.

B.5. Single-step distillation methods comparison

Table 6 justifies our choice of DMD/DMD2 as our first-stage training without adversarial loss. Competitor methods either

Table 4: CLIP score comparison for high guidance scale on MS-COCO2014. LCM-LoRA is trained with a classifier-free guidance (CFG) scale of 7.5, while other methods use a CFG of 8.

Method	Latency (↓)	CLIP score (↑)
DPM++ (4 step) (Lu et al., 2022b)	0.26s	0.309
UniPC (4 step) (Zhao et al., 2024)	0.26s	0.308
LCM-LoRA (1 step) (Luo et al., 2023)	0.09s	0.238
LCM-LoRA (4 step) (Luo et al., 2023)	0.19s	0.297
DMD2 (our reimplementation) (Yin et al., 2024a)	0.09s	0.306
MSD4-ADM (ours)	0.09s	0.308
DMD (Yin et al., 2024b)	0.09s	0.320
SDv1.5 (teacher) (Rombach et al., 2022)	2.59s	0.322

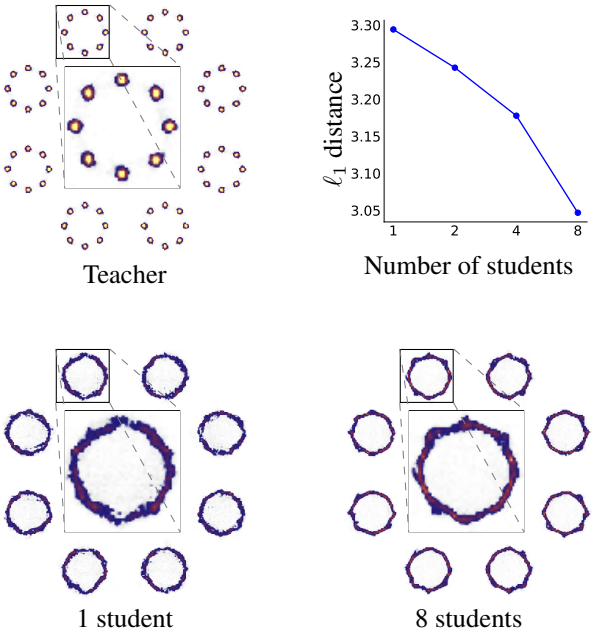

Figure 5: A 2D toy model using consistency distillation. From left to right: teacher (multi-step) generation and student, one-step generation with 1 and 8 distilled students, the ℓ_1 distance of generated samples between teacher and students. **Takeaway:** More students improve distillation quality on this easy-to-visualize setup with consistency distillation.

need larger training data size (EMD, SiD) or have worse quality (CTM and other CM-based methods). DMD/DMD2, on the other hand, strike a good balance. DMD exhibits more stability for MSD on ImageNet, whereas DMD2 performs better for SD v1.5, which leads to our respective choices. As mentioned in App. D, we used a smaller-sized paired dataset (10 000 images) than the original DMD paper (25 000 images) for ImageNet, which significantly accelerated convergence without impairing the final performance. Moreover, as in Sec. 3.2, the same paired dataset can be used for all students, eliminating potential additional computation.

Table 5: Ablation studies on different components of MSD. All experiments are done on ImageNet-64×64, trained with only the DM stage for 20k iterations, where B is the batch size per student. See App. B.3.

Method	FID (↓)
4 students, $B = 32$	2.53
1 students, $B = 128$	2.60
2 students, $B = 128$	2.49
4 students, B = 128 (baseline)	2.37
8 students, $B = 128$	2.32
4 students, $B = 128$, K-means splitting	2.39
4 students, $B = 128$, random splitting	2.45

B.6. More results on distilling into smaller students

In Sec. 4.1, we trained MSD4-ADM on smaller students to demonstrate the tradeoff between generation quality and speed. Here, we make a more comprehensive ablation study on the interplay between student size, number of classes covered, and training stage, with results in Fig. 8. We observe that generation quality increases with student size and decreases with more classes covered. MSD offers great flexibility for users to make these choices based on computational resources, generation quality, and inference speed requirements.

C. Deployment suggestions

Here, we discuss some MSD deployment options for practitioners.

A naive option for deployment is to use increased GPU memory to host all models simultaneously. However, this is impractical and wasteful, as only a single student model needs to be used for each user request. In settings with less GPU memory than all students' sum memory requirement, we must swap student models on and off GPUs. This incurs extra latency. However, in the few-GPU many-users setting, there are already prominent latency issues, such as users needing to queue for usage. In few-user settings, resources are likely being taken offline to save cost, and thus, there

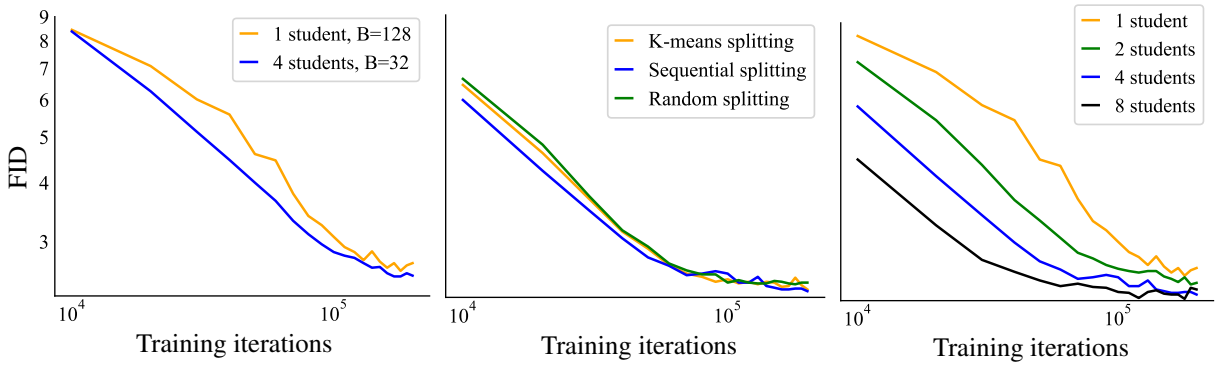

Figure 6: FID comparisons during training for ablations in Table 5

.

Table 6: Comparison of various aspects of single-step distillation methods.

Method on ImageNet	Terminal FID	Iterated Images
DMD (Yin et al., 2024b) (our reimplementation)	2.54	$\sim$ 130M
DMD2 (w/o GAN) (Yin et al., 2024a)	2.61	$\sim$ 110M
EMD (Xie et al., 2024a)	2.20	$\sim$ 600M
SiD ($\alpha = 1.0$) (Zhou et al., 2024)	2.02	$\sim$ 500M
CTM (Kim et al., 2024)	>5	$\sim$ 3M

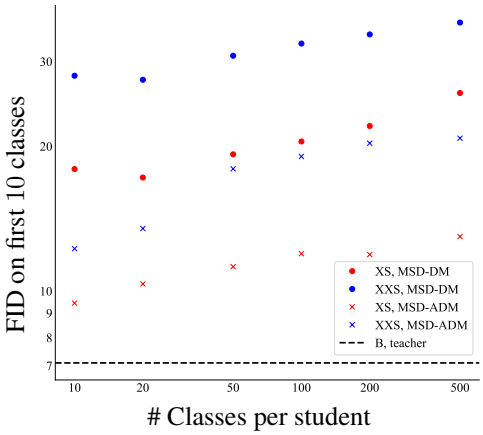

Figure 8: The effect of student size, number of classes covered, and training stage on the performance of a single smaller student. XS, XXS, and B refer to model sizes, with precise definitions provided in Tab. 7. Also, see special evaluation details in App. E.

is start-up latency for fresh requests, too. Therefore, we argue that the more interesting setting is in large distributed deployment.

For settings with more GPU memory than all students' sum memory requirements, we can distribute the student models among a cluster of GPUs (as one would the teacher) and route each generation request to the appropriate student node. The routing layer is lightweight compared to the inference cost, so we pay little for it.

If the data has been partitioned uniformly according to user demand, the incoming requests will be distributed uniformly among the student nodes. Therefore, we achieve equal throughput compared to the teacher without more overall model storage. However, finding such a partition is challenging, and user demand may change over time. This leaves finding the optimal allocation of resources to the student nodes an open problem. In practice, we expect that a reduced student model size would lead to an overall reduction in storage requirements compared to the teacher alone.

D. Implementation Details

D.1. Toy Experiments

The real dataset is a mixture of Gaussians. The radius for the outer circle is 0.5, the radius for the 8 inner circles is 0.1, and the standard deviation for each Gaussian (smallest circle) is 0.005. The teacher is trained with EDM noise schedule, where use $(\sigma_{\min}, \sigma_{\max}) = (0.002, 80)$ and discretized the noise schedule into 1000 steps. We train the teacher for 100 000 iterations with AdamW (Loshchilov, 2017) optimizer, setting the learning rate at 1e-4, weight decay to 0.01, and beta parameters to $(0.9, 0.999)$. For distillation, we first generated a dataset of 1000 pairs, then used DMD (Yin et al., 2024b) to train 1, 2, 4, and 8 students, respectively, all for 200 000 iterations, with reduced learning rate at 1e-7. We only sample the first 750 of the 1000 steps for distillation.

Each subfigure of Fig. 4 is a histogram with 200 bins on 100 000 generated samples, using a custom colormap. The

loss is the mean absolute difference of binned histogram values.

D.2. ImageNet

D.2.1. Same-sized students

Our ImageNet experiments setup closely follows DMD (Yin et al., 2024b) and DMD2 (Yin et al., 2024a) papers. We distill our one-step generators using the EDM (Karras et al., 2022) checkpoint "edm-imagenet-64x64-cond-adm". We use $\sigma_{\min} = 0.002$ and $\sigma_{\max} = 80$ and discretize the noise schedules into 1000 bins. The weight w_t in Eq. (6) is set to $\frac{\sigma_t^2}{\alpha_t} \frac{CS}{\|\boldsymbol{\mu}_{\text{teacher}}(\boldsymbol{x}_t,t)-\boldsymbol{x}\|_1}$ where S is the number of spatial locations and C is the number of channels, and the weight λ_t in Eq. (8) is set to $(\sigma_t^2 + 0.5^2)/(\sigma_t \cdot 0.5)^2$.

For the DM stage, we prepare a distillation dataset by generating 10 000 noise-image pairs using the deterministic Heun sampler (with $S_{\text{churn}} = 0$ over 256 steps. We use the AdamW optimizer (Loshchilov, 2017) with learning rate 2e-6, weight decay 0.01, and beta parameters $(0.9, 0.999)$. We compute the LPIPS loss using a VGG backbone from the LPIPS library (Zhang et al., 2018), and we upscale the image to 224×224 using bilinear upsampling. The regression loss weight is set to 0.25. We use mixed-precision training and a gradient clipping with an ℓ_2 norm of 10. We partition the 1000 total classes into consecutive blocks of 250 classes and trained 4 specialized students using $\text{Distill}_{\text{DM}}$ and F_{DM} defined in Sec. 2. Each student is trained on 4 A100 GPUs, with a total batch size of 128, for 200 000 iterations. This yields the MSD4-DM checkpoint in Tab. 1.

For the ADM stage, we attach a prediction head to the middle block of the fakescore model. The prediction head consists of a stack of 4×4 convolutions with a stride of 2, group normalization, and SiLU activations. All feature maps are downsampled to 4×4 resolution, followed by a single convolutional layer with a kernel size and stride of 4. The final output linear layer maps the given vector to a scalar predicted probability. We load the best generator checkpoint from DM stage but re-initialize the fakescore and GAN classifier model from teacher weights, as we observed this leads to slightly better performance. We set the GAN generator loss weight to 3e-3 and the GAN discriminator loss weight to 1e-2 and reduce the learning rate to 5e-7. Each student is trained on 4 A100 GPUs, with a total batch size of 192, for 150 000 iterations. This yields the MSD4-ADM checkpoint in Tab. 1.

D.2.2. Smaller students

Following a minimalist design, we pick our smaller student's architecture by changing hyperparameter values of the "edm-imagenet-64x64-cond-adm" checkpoint architecture. See details in Tab. 7.

For the MSD4-ADM-S checkpoint in Tab. 1, we train the TSM stage using the model architecture S with the continuous EDM noise schedule with $(P_{\text{mean}}, P_{\text{std}}) = (-1.2, 1.2)$ and the weighting $\lambda_t = (\sigma_t^2 + 0.5^2)/(\sigma_t \cdot 0.5)^2$. We use a learning rate of 1e-4. Each student is trained on 4 A100 GPUs, with a total batch size of 576, for 400 000 iterations. Then DM and ADM stages were trained using a total batch size of 160, following otherwise the same setup as Sec. D.2.1.

For the ablation study in B.6, we instead train a common TSM stage for all students for computational efficiency. We train this common stage using 16 A100 GPUs, with a total batch size of 3584 and 4864 for architecture XS and XXS, respectively. The DM and ADM stages are followed by specialized students with filtered data and 4 A100 GPUs each, with a total batch size of 224 and 256 for architecture XS and XXS, respectively, and using the same learning rate of 2e-6.

D.3. SD v1.5

D.3.1. Same-sized students, CFG=1.75

Our SD v1.5 experiments setup closely follows DMD2 (Yin et al., 2024a) paper. We distill our one-step generators from the SD v1.5 (Rombach et al., 2022) model, using a classifier-free guidance scale of 1.75 for the teacher model to obtain the best FID score. We use the first 5M prompts from the COYO dataset (Byeon et al., 2022) and the corresponding 5M images for the GAN discriminator. We apply the DDIM noise schedule with 1000 steps for sampling t. The weight w_t in Eq. 6 is set to $\frac{\sigma_t^2}{\alpha_t} \frac{CS}{\|\boldsymbol{\mu}_{\text{teacher}}(\boldsymbol{x}_t,t)-\boldsymbol{x}\|_1}$ where S is the number of spatial locations and C is the number of channels, and the weight λ_t in Eq. 8 is set to α_t^2/σ_t^2.

For the DM stage, we use the AdamW optimizer (Loshchilov, 2017) with learning rate 1e-5, weight decay 0.01, and beta parameters $(0.9, 0.999)$. We use gradient checkpointing, mixed-precision training, and a gradient clipping with an ℓ_2 norm of 10. We partition the prompts and corresponding images by the 4 quadrants formed by the first 2 entries of the embeddings, where the embeddings are pooled from the outputs of the SD v1.5 text embedding layers. We choose not to include a regression loss but instead use a TTUR, which updates the fakescore model 10 times per generator update. Each of the 4 students is trained on 32 A100 GPUs, with a total batch size of 1536, for 40 000 iterations. This yields the MSD4-DM checkpoint in Tab. 2.

For the ADM stage, we attach a prediction head that has the same architecture (though with a different input size) as Sec. D.2. We load both the best generator checkpoint and the corresponding fakescore checkpoint from DM stage. We set the GAN generator loss weight to 1e-3 and the GAN discriminator loss weight to 1e-2 and reduced the learning

Table 7: Hyperparameter details for different sized student models of the ADM architecture. Unspecified hyperparameters remain the same as the teacher. Latency is measured on a single NVIDIA RTX 4090 GPU.

Model Identifier	# Channels	Channel Multipliers	# Residual Blocks	# Parameters	Latency
B (teacher)	192	$[1, 2, 3, 4]$	3	296M	0.0271s
S	160	$[1, 2, 2, 4]$	3	173M	0.0253s
XS	128	$[1, 2, 2, 4]$	2	86M	0.0209s
XXS	96	$[1, 2, 2, 2]$	2	26M	0.0192s

rate to 5e-7. Each student is trained on 32 A100 GPUs, with a total batch size of 1024, for 5000 iterations. This yields the MSD4-ADM checkpoint in Tab. 2.

D.3.2. Same-sized students, CFG=8

The above CFG $= 1.75$ setting yields sub-optimal image quality. Similar to previous works (Yin et al., 2024b; Lin et al., 2024; Rombach et al., 2022), we choose CFG $= 8$ for enhanced image quality. Due to time and computational resource limitations, we only train with the ADM stage. Each of the 4 students is trained on 32 A100 GPUs, with a learning rate of 1e-5 and a batch size of 1024 for both the fake and the real images, for 6000 iterations. This yields the checkpoint that is used to generate Fig. 3 (b) and Fig .14. Longer training with the added DM stage can likely further improve the generation quality.

D.3.3. Smaller student, CFG=8

We again pick our smaller student's architecture by changing the hyperparameter values of the SD v1.5 architecture. See details in Tab. 8.

To create a subset of dog-related data, we first selected $\sim$ 1 210 000 prompts in the COYO (Byeon et al., 2022) dataset whose embeddings are closest to "a dog." We then created an equal number of noise-image pairs from the SD v1.5 teacher using these prompts with CFG $= 8$. We train the TSM stage using the model architecture S with the 1000-step DDIM noise schedule and the weighting $\lambda_t = \alpha_t^2/\sigma_t^2$. We use a learning rate of 1e-4. We then continue to the DM stage with the paired regression loss, using a learning rate of 1e-5, and finally continue to the ADM stage using generated paired images as "real" images with a learning rate of 5e-7. We use 16 A100 GPUs. The TSM stage is trained with a total batch size of 1536 for 240 000 iterations. The DM stage is trained with a total batch size of 512 for both the paired and the fake images for 20 000 iterations, and the ADM stage is trained with the same batch size for 6000 iterations. This yields the checkpoint used to generate Fig. 3(c). Longer training and better tuning are again likely to improve the generation quality further.

D.4. SDXL

Our SDXL experiments setup also closely follows DMD2 (Yin et al., 2024a) paper. We set the conditioning timestep to 399 and pretrain a common student with a regression loss using 10K pairs for 2000 iterations. We then proceed directly to the ADM state with a learning rate of 5e-7, setting the GAN generator loss weight to 5e-3 and the GAN discriminator loss weight to 1e-2. For each of the 4 general student, we use 64 A100 GPUs, setting the total batch size to 128 and trains for 24 000 iterations. For the specialized "cat" student, we train on a subset of the COYO dataset whose embeddings are closest to "a cat."

E. Evaluation Details

For zero-shot COCO evaluation, we use the exact setup as GigaGAN (Yu et al., 2022) and DMD2 (Yin et al., 2024a). Specifically, we generate 30 000 images using the prompts provided by DMD2 code. We downsample the generated images using PIL to 256×256 Lanczos resizer. We then use the clean-fid (Parmar et al., 2022) to compute the FID score between generated images and 40 504 real images from the COCO 2014 validation dataset. Additionally, we use the OpenCLIP-G backbone to compute the CLIP score. For ImageNet, we generate 50 000 images and calculate FID using EDM (Karras et al., 2022) evaluation code. When selecting the best checkpoints for partitioned students, the same procedure is applied only for prompts/classes within respective partitions. For the ablation study in Sec. B.6, 10 000 images are generated for only the first 10 classes for an apple-to-apple comparison.

F. Additional qualitative results

F.1. Additional Imagenet-64×64 results

In Fig. 9, we present ImageNet-64×64 generations from the teacher and different sized students to support the claims in Sec. 4.1.

In Fig. 12, we present more ImageNet-64×64 qualitative results collectively generated by our 4 same-sized students trained with MSD-ADM. In Fig. 13, we display corresponding generations from 4 smaller students with architecture S (see Tab. 7).

Table 8: Hyperparameter details for different sized student models of the SD v1.5 architecture. Only the diffusion model part is measured since the text encoder and the VAE remain frozen. Unspecified hyperparameters remain the same as the teacher. Latency is measured on a single NVIDIA RTX 4090 GPU.

Model Identifier	# block_out_channels	# Parameters	Latency
B (teacher)	[320, 640, 1280, 1280]	860M	0.041s
S	[160, 320, 320, 640]	142M	0.039s

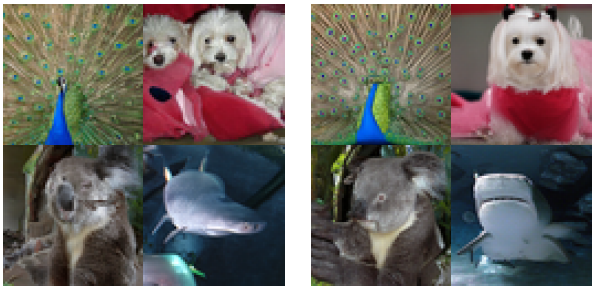

(a) Teacher (multistep) (b) Same-sized students

(b) 42% smaller students (b) 71% smaller students

Figure 9: Sample generations on ImageNet-64×64 from the multistep teacher and different sized students, with architecture and latency details in App. D. The same-size students have comparable or slightly better generation quality than the teacher. Smaller students achieve faster generation while still having decent qualities. Same-sized students are trained with DM and ADM stages, whereas smaller students are trained with all three stages (see Fig. 2).

Teacher (multistep)

Figure 10: Sample generations from the SD v1.5 teacher (see details in Fig. 3).

(a) General students (b) Specialized student

Figure 11: High resolution samples on high guidance-scale text-to-image generations from students distilled from the SDXL teacher, with full training details in App. D. The specialized student focusing on cat-related prompts has comparable or better qualities than general students.

F.2. Additional Text-to-image Synthesis Results

In Fig. 10, we present generations from the SD v1.5 teacher to complement the results in Fig. 3.

In Fig. 11, we present generations from the general SDXL students trained on all COYO prompts, and a specialized student trained on cat-related prompts. We observe the specialized student has comparable or sometimes better qualities (i.e. fixes the multi-tail problem) than general students, indicating a better use of effective capacity.

In Fig. 14, and Fig. 16, we present more qualitative results collectively generated by out 4 students trained on the COYO dataset with MSD-ADM, from the SD v1.5 teacher and the SDXL teacher, respectively. These students are trained with a teacher classifier-free guidance (CFG) scale of 8.

G. Prompt details

G.1. Prompts for Fig. 14

We use the following prompts for Fig. 14, from left to right, top to bottom:

- wise old man with a white beard in the enchanted and magical forest
- a high-resolution photo of an orange Porsche under sunshine

- Astronaut on a camel on mars
- a hot air balloon in shape of a heart. Grand Canyon
- transparent vacation pod at dramatic scottish lochside, concept prototype, ultra clear plastic material, editorial style photograph
- penguin standing on a sidewalk
- border collie surfing a small wave, with a mountain on background
- an underwater photo portrait of a beautiful fluffy white cat, hair floating. In a dynamic swimming pose. The sun rays filters through the water. High-angle shot. Shot on Fujifilm X
- 3D animation cinematic style young caveman kid, in its natural environment
- robot with human body form, robot pieces, knolling, top of view, ultra realistic
- 3D render baby parrot, Chibi, adorable big eyes. In a garden with butterflies, greenery, lush, whimsical and soft, magical, octane render, fairy dust
- a chimpanzee sitting on a wooden bench
- a capybara made of voxels sitting in a field
- a cat reading a newspaper
- a squirrell driving a toy car
- close-up photo of a unicorn in a forest, in a style of movie still

G.2. Prompts for Fig. 16

We use the following prompts for Fig. 16, from left to right, top to bottom:

- a teddy bear on a skateboard in times square
- a portrait of a statue of the Egyptian god Anubis wearing aviator goggles, white t-shirt and leather jacket. The city of Los Angeles is in the background.
- A soft beam of light shines down on an armored granite wombat warrior statue holding a broad sword. The statue stands an ornate pedestal in the cella of a temple. wide-angle lens. anime oil painting.
- A still image of a humanoid cat posing with a hat and jacket in a bar.
- A close-up of a woman's face, lit by the soft glow of a neon sign in a dimly lit, retro diner, hinting at a narrative of longing and nostalgia.
- A television made of water that displays an image of a cityscape at night.
- a capybara made of voxels sitting in a field
- a portrait of an old man

G.3. Prompts for Fig. 15

We use the following prompts for Fig. 15, from left to right, top to bottom:

- a squirrell driving a toy car
- a giant gorilla at the top of the Empire State Building
- a goat wearing headphones
- A photo of an astronaut riding a horse in the forest.
- an elephant walking on the Great Wall
- a watermelon chair
- An oil painting of two rabbits in the style of American Gothic, wearing the same clothes as in the original.
- A photograph of the inside of a subway train. There are red pandas sitting on the seats. One of them is reading a newspaper. The window shows the jungle in the background.

G.4. Prompts for Fig. 3

We use the following prompts (same for all three models), from left to right, top to bottom:

- dog on a bed
- Your Puppy Your Dog
- Trained Happy Dog
- Very handsome dog.

G.5. Prompts for Fig. 11

We use the following prompts (same for two cases), from left to right, top to bottom:

- A majestic Persian cat lounging on a royal velvet cushion.
- A playful kitten chasing a butterfly in a flower field.
- A grumpy gray cat wearing a small bow tie and glasses.
- A fluffy orange tabby cat sitting on a sunny windowsill.

H. Related Work

Diffusion sampling acceleration. While a line of work aims to accelerate diffusion models via fast numerical solvers for the PF-ODE (Lu et al., 2022a;b; Zheng et al., 2024; Karras et al., 2022; Liu et al., 2022), they usually still require more than 10 steps. Training-based methods that usually follow the knowledge distillation pipeline can achieve few-step or even one-step generation. Luhman and Luhman (2021) first used the diffusion model to generate a noise and image pair dataset that is then used to train a single-step generator. DSNO (Zheng et al., 2023) precomputes the denoising trajectory and uses neural operators to estimate the whole PF-ODE path. Progressive distillation (Salimans and Ho, 2022; Meng et al., 2023) iteratively halves the number of sampling steps required without needing an offline dataset. Rectified Flow (Liu et al., 2023b) and follow-up works (Liu et al., 2023a; Yan et al., 2024) straighten the denoising trajectories to allow sampling in fewer steps. Another approach uses self-consistent properties of denoising trajectories to inject additional regularization for distillation (Song et al., 2023; Luo et al., 2023; Ren et al., 2024; Kim et al., 2024).

The methods above require the student to follow the teacher's trajectories. Instead, a recent line of works aims to only match the distribution of the student and teacher output via variational score distillation (Yin et al., 2024b;a; Salimans et al., 2024; Xie et al., 2024a; Luo et al., 2024; Zhou et al., 2024; Nguyen and Tran, 2024). The adversarial loss (Goodfellow et al., 2014), often combined with the above techniques, has been used to enhance the distillation performance further (Xiao et al., 2022; Zheng and Yang, 2024; Sauer et al., 2023b; 2024; Wang et al., 2023; Xu et al., 2024; Lin et al., 2024; Kim et al., 2024). Although MSD is conceptually compatible and offers a performance boost to all of these distillation methods, in this work, we demonstrate two specific techniques: distribution matching (Yin et al., 2024b) and adversarial distillation (Yin et al., 2024a).

Mixture of experts training and distillation. Mixture of Experts (MoE), first proposed in (Jordan and Jacobs, 1994), has found success in training very large-scale neural networks (Shazeer et al., 2017; Lepikhin et al., 2021; Fedus et al., 2022; Lewis et al., 2021; Borde et al., 2024). Distilling a teacher model into multiple students was explored by Hinton et al. (2015), and after that, has been further developed for supervised learning (Chen et al., 2020; Ni and Hu, 2023; Chang et al., 2022) and language modeling (Xie et al., 2024b; Kudugunta et al., 2021; Zuo et al., 2022). Although several works (Hoang et al., 2018; Park et al., 2018; Ahmetoğlu and Alpaydın, 2021) have proposed MoE training schemes for generative adversarial networks, they train the MoE from scratch. This requires carefully tuning the multi-expert adversarial losses. eDiff-I (Balaji et al., 2022) uses different experts in different denoising timesteps for a multi-step diffusion model. However, to the best of our knowledge, MSD is the first method to *distill* multi-step teacher diffusion models into multiple one-step students for image generation.

Efficient architectures for diffusion models. In addition to reducing steps, an orthogonal approach aims to accelerate diffusion models with more efficient architectures. A series of works (Bao et al., 2022; Peebles and Xie, 2023; Hoogeboom et al., 2023) introduces vision transformers to diffusion blocks and trains the diffusion model with new architectures from scratch. Another line of work selectively removes or modifies certain components of a pretrained diffusion model and then either finetunes (Kim et al., 2023; Li et al., 2024; Zhang et al., 2024) or re-trains (Zhao et al., 2023) the lightweight diffusion model, from which step-distillation can be further applied (Li et al., 2024; Zhao et al., 2023). Our approach is orthogonal to these works in two regards: 1) In our method, each student only handles a subset of data, providing a gain in relative capacity. 2) Instead of obtaining a full diffusion model, our method employs a lightweight pretraining stage to obtain a good initialization for single-step distillation. Combining MSD with more efficient architectures is a promising future direction.

I. Preliminary

We introduce the background on diffusion models in Sec. I.1 and distribution matching distillation (DMD) in Sec. I.2. We discuss applying adversarial losses to improve distillation in Sec. I.3.

I.1. Diffusion Models

Diffusion models learn to generate data by estimating the score functions (Song et al., 2021) of the corrupted data distribution on different noise levels. Specifically, at different timesteps t, the data distribution p_{real} is corrupted with an independent Gaussian noise: $p_{t,\text{real}}(\boldsymbol{x}_t) = \int p_{\text{real}}(\boldsymbol{x}) q_t(\boldsymbol{x}_t|\boldsymbol{x}) d\boldsymbol{x}$ where $q_t(\boldsymbol{x}_t|\boldsymbol{x}) \sim \mathcal{N}(\alpha_t \boldsymbol{x}, \sigma_t^2 \boldsymbol{I})$ with predetermined α_t, σ_t following a forward diffusion process (Song et al., 2021; Ho et al., 2020). The neural network learns the score of corrupted data $\boldsymbol{s}_{\text{real}} := \nabla_{\boldsymbol{x}_t} \log p_{t,\text{real}}(\boldsymbol{x}_t) = -(\boldsymbol{x}_t - \alpha_t \boldsymbol{x})/\sigma_t^2$ by equivalently predicting the denoised $\boldsymbol{x}$: $\boldsymbol{\mu}(\boldsymbol{x}_t, t) \approx \boldsymbol{x}$. After training with the denoising score matching loss $\mathbb{E}_{\boldsymbol{x},t,\boldsymbol{x}_t}[\lambda_t \|\boldsymbol{\mu}(\boldsymbol{x}_t, t) - \boldsymbol{x}\|_2^2]$, where λ_t is a weighting coefficient, the model generates the data by an iterative denoising process over a decreasing sequence of time steps.

I.2. Distribution Matching Distillation

Inspired by Wang et al. (2024), the works of Luo et al. (2024); Yin et al. (2024b); Ye and Liu (2024); Nguyen and Tran (2024) aim to train the single-step distilled student to match the generated distribution of the teacher diffusion model. This is done by minimizing the following reverse KL divergence between teacher and student output distributions, diffused at different noise levels for better support over the

ambient space:

$$\mathbb{E}_t D_{\mathrm{KL}}(p_{t,\text{fake}} \| p_{t,\text{real}}) = \mathbb{E}_{\boldsymbol{x}_t}\left(\log\left(\frac{p_{t,\text{fake}}(\boldsymbol{x}_t)}{p_{t,\text{real}}(\boldsymbol{x}_t)}\right)\right). \quad (5)$$

The training only requires the gradient of Eq. (5), which reads (with a custom weighting w_t):

$$\begin{aligned}&\nabla_\theta \mathcal{L}_{\mathrm{KL}}(\theta) := \nabla_\theta \mathbb{E}_t D_{\mathrm{KL}} \\ &\simeq \mathbb{E}_{\boldsymbol{z},t,\boldsymbol{x}_t}[w_t \alpha_t (\boldsymbol{s}_{\text{fake}}(\boldsymbol{x}_t, t) - \boldsymbol{s}_{\text{real}}(\boldsymbol{x}_t, t)) \nabla_\theta G_\theta(\boldsymbol{z})],\end{aligned} \quad (6)$$

where $\boldsymbol{z} \sim \mathcal{N}(0, \boldsymbol{I}), t \sim \text{Uniform}[T_{\min}, T_{\max}]$, and $\boldsymbol{x}_t \sim q(\boldsymbol{x}_t|\boldsymbol{x})$, the noise injected version of $\boldsymbol{x} = G_\theta(\boldsymbol{z})$ generated by the one-step student. Here, we assume the teacher denoising model accurately approximates the score of the real data, and a "fake" denoising model approximates the score of generated fake data:

$$\begin{aligned}\boldsymbol{s}_{\text{real}}(\boldsymbol{x}_t, t) &\approx -(\boldsymbol{x}_t - \alpha_t \boldsymbol{\mu}_{\text{teacher}}(\boldsymbol{x}_t, t))/\sigma_t^2, \\ \boldsymbol{s}_{\text{fake}}(\boldsymbol{x}_t, t) &\approx -(\boldsymbol{x}_t - \alpha_t \boldsymbol{\mu}_{\text{fake}}(\boldsymbol{x}_t, t))/\sigma_t^2.\end{aligned} \quad (7)$$

The "fake" denoising model is trained with the denoising objective with weighting λ_t:

$$\mathcal{L}_{\text{denoise}}(\phi) = \mathbb{E}_{\boldsymbol{z},t,\boldsymbol{x}_t}[\lambda_t \|\boldsymbol{\mu}^{\phi}_{\text{fake}}(\boldsymbol{x}_t, t) - \boldsymbol{x}\|_2^2]. \quad (8)$$

The generator and the "fake" denoising model are updated alternatively. To facilitate better convergence of the KL divergence, Distribution Matching Distillation (DMD) and DMD2 (Yin et al., 2024a) used two distinct strategies, both significantly improving the generation performance. DMD proposes to complement the KL loss with a regression loss to encourage mode covering:

$$\mathcal{L}_{\text{reg}}(\theta) = \mathbb{E}_{(\boldsymbol{z},y)\sim\mathcal{D}_{\text{paired}}} \ell(G_\theta(\boldsymbol{z}), y), \quad (9)$$

where $\mathcal{D}_{\text{paired}}$ is a dataset of latent-image pairs generated by the teacher model offline, and ℓ is the Learned Perceptual Image Patch Similarity (LPIPS) (Zhang et al., 2018). DMD2 instead applies a two-timescale update rule (TTUR), where they update the "fake" score model for N steps per generator update, allowing more stable convergence. We use distribution matching (DM) to refer to all relevant techniques introduced in this section.

I.3. Enhancing distillation quality with adversarial loss

The adversarial loss, originally proposed by Goodfellow et al. (2014), has shown a remarkable capability in diffusion distillation to enhance sharpness and realism in generated images, thus improving generation quality. Specifically, DMD2 (Yin et al., 2024a) proposes adding a minimal discriminator head to the bottleneck layer of the "fake" denoising model μ_{fake}, which is naturally compatible with DMD's alternating training scheme and the TTUR. Moreover, they showed that one should first train the model without GAN to convergence, then add the GAN loss and continue training. This yields better terminal performance than training with the GAN loss from the beginning. We use adversarial distribution matching (ADM) to refer to distribution matching with added adversarial loss.

J. Extended Discussion

J.1. Limitations

MSD is the first work to explore diffusion distillation with multiple students, and it admits a few limitations that call for future work. 1) Further explorations could offer more insights into optimal design choices for a target quality and latency on various datasets, such as the number of students, input condition size for each student, and other hyperparameters. This is especially beneficial if the training budget is limited. 2) We apply simple partitioning for both class- and text-conditions and assign them disjointly to different students. Although our empirical study shows that simple alternatives do not offer obvious advantages, more sophisticated routing mechanisms may help. 3) We use simple channel reduction when designing smaller students to demonstrate feasibility. This results in a significantly smaller latency reduction than sample size reduction. Exploring other designs of smaller students will likely increase their quality and throughput. 4) We train different students separately, but we expect that carefully designed weight-sharing, loss-sharing, or other interaction schemes can further enhance training efficiency. 5) We hypothesize that MSD can be applied to other diffusion distillation methods and other modalities for similar benefits, but leave this for future work.

Figure 12: Collective one-step samples from 4 same-sized students trained with MSD-ADM on ImageNet (FID = 1.20).

Figure 13: Collective one-step samples from 4 smaller students trained with MSD-ADM on ImageNet (FID = 2.88).

Figure 14: Collective one-step samples from 4 SD v1.5 students trained with MSD-ADM on COYO with CFG = 8.

Figure 15: Additional collective one-step samples from 4 SDXL students trained with MSD-ADM on COYO with CFG $= 8$.

Figure 16: Collective one-step 1024×1024 samples from 4 SDXL students trained with MSD.